

Weibull Analysis of Mechanical Data for Castings II: Weibull Mixtures and Their Interpretation

MURAT TIRYAKIOĞLU

The interpretation of Weibull probability plots of mechanical testing data from castings was discussed in Part 1 (M. Tiryakioğlu, J. Campbell: Metall. Mater. Trans. A, 41 (2010) 3121-3129). In Part II, details about the mathematical models of Weibull mixtures are introduced. The links between the occurrence of Weibull mixtures and casting process parameters are discussed. Worked examples are introduced in five case studies in which six datasets from the literature were reanalyzed. Results show that tensile and fatigue life data should be interpreted differently. In tensile data, Weibull mixtures are due to two distinct defect distributions, namely “old” and “young” bifilms, which are a result of prior processing and mold filling, respectively. “Old” bifilms are the predominant defect and result in the lower distribution, whereas “young” bifilms results on the upper distribution. In fatigue life data, Weibull mixtures are due to two failure mechanisms being active: failure due to cracks initiating from surface defects and interior defects. Surface defects are predominant and interior defects lead to fatigue failure only when there are no cracks initiated by surface defects. In all cases, only the mutually exclusive Weibull mixture model was found to be applicable.

DOI: 10.1007/s11661-014-2610-9

© The Minerals, Metals & Materials Society and ASM International 2014

I. INTRODUCTION

THE Griffith theory of brittle fracture requires a preexisting crack to initiate failure.^[1] Similarly, ductile fracture requires a population of pores or cracks.^[2,3] Consequently, statistical models for fracture in materials are all built on the concept that the difference between the ideal and actual performances can be attributed to the presence of defects (flaws) raising local stresses, and consequently, resulting in premature failure. Hence the statistical distributions of fracture-related mechanical properties, such as fracture stress, elongation, impact, fracture toughness, fatigue life, *etc.*, can all be linked to the underlying defect size distribution. Statistically, this implies that the worst (largest) defect leading to the highest stress concentration is the one that determines the fracture-related mechanical properties.^[4] Hence this defect constitutes the “weakest link”, based on the theory developed by Pierce.^[5] The “weakest link” theory applies in situations that are analogous to the failure of a chain when its weakest link has failed.^[6] Based on the “weakest link” theory, Weibull^[7] introduced an empirical distribution, for which the cumulative probability function is expressed as:

$$P = 1 - \exp\left[-\left(\frac{\sigma - \sigma_T}{\sigma_0}\right)^m\right], \quad [1]$$

where P is the probability of failure at a given stress (strain, fatigue life, *etc.*), σ , or lower. The threshold

value, σ_T , is the value below which no specimen is expected to fail. The term, σ_0 , is the scale parameter, and m is the shape parameter, alternatively referred to as the Weibull modulus. The probability density function, f , for any continuous distribution is found by:

$$f = \frac{dP}{d\sigma} \quad [2a]$$

For the Weibull distribution, f is expressed as:

$$f = \frac{m}{\sigma_0} \left(\frac{\sigma - \sigma_T}{\sigma_0}\right)^{m-1} \exp\left[-\left(\frac{\sigma - \sigma_T}{\sigma_0}\right)^m\right] \quad [2b]$$

One of the most commonly used methods of presenting the Weibull fits to data is the Weibull probability plot. After rearranging, Eq. [1] can be written as

$$\ln[-\ln(1 - P)] = m \ln(\sigma - \sigma_T) - m \ln(\sigma_0) \quad [3]$$

Note that Eq. [3] has a linear form when the left-hand side of the equation is plotted vs $\ln(\sigma - \sigma_T)$ with a slope of m and an intercept of $-m \ln(\sigma_0)$. Alternatively, the Weibull probability plot can be obtained when the left-hand side of the equation is plotted vs $\ln(\sigma)$. This method of presentation gives a straight line relationship only when $\sigma_T = 0$. This is demonstrated in Figure 1, in which Weibull distributions for three datasets for tensile strength (S_T) of sand cast A356^[8,9] are plotted. Probability was assigned to each data point by using the following plotting position formula:

$$P = \frac{i - 0.5}{n}, \quad [4]$$

where i is the rank in ascending order and n is the sample size. Note that the trend of the curve at low values of $\ln(\sigma)$ is

MURAT TIRYAKIOĞLU, Director, is with the School of Engineering, University of North Florida, 1 UNF Drive, Jacksonville, FL 32224. Contact e-mail: m.tiryakioglu@unf.edu

Manuscript submitted June 26, 2014.

Article published online October 21, 2014

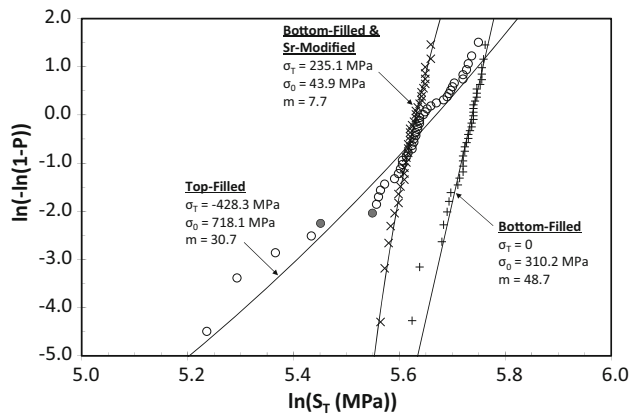


Fig. 1—The Weibull probability plots for the tensile strength of A356 aluminum castings by Green and Campbell.^[8,9] The best 3-parameter Weibull fits are also indicated.

influenced by the value of the threshold, σ_T ; a positive threshold, as in the “bottom-filled and Sr-modified” castings, results in higher slope at low values of $\ln(\sigma)$. For “bottom-filled” castings, the threshold value is zero, and consequently the best-fit trend is a straight line. When the threshold is negative however, as in the “top-filled” castings, the slope decreases with decreasing $\ln(\sigma)$. For mechanical properties, a negative threshold is, of course, meaningless. In Part I,^[10] recommendations on how to interpret the Weibull probability plots of mechanical data from castings were provided; it was suggested that a negative threshold is a strong indication of the presence of multiple Weibull distributions, *i.e.*, Weibull mixture. This paper introduces two different scenarios for Weibull mixtures along with worked examples* by using data from the literature.

*All estimated Weibull parameters for the datasets were obtained by using the maximum likelihood method.

II. WEIBULL MIXTURE MODELS

A. Mathematical Treatment

As indicated above, a negative threshold in a 3-parameter Weibull fit to fracture-related mechanical data in castings is evidence for the presence of a Weibull mixture. Further evidence is that the slope in a probability plot (i) decreases significantly, or (ii) approaches zero and then increases again,^[11] like an inflection point, as observed in the data from the top-filled castings in Figure 1; the filled circles indicate the location of the inflection point in the trend of the data. The 3-parameter fit, of course, does not show any inflection point.

When these discernments are exercised, it can be observed that Weibull mixtures are not uncommon in castings.^[10] An example was provided by Cox *et al.*^[12] who investigated the effect of top and bottom filling in investment castings with different alloys. We will focus on the results for Ni alloy IN939 castings. For bottom-filled castings, a 20 ppi (pores per inch) ceramic foam filter was incorporated into the filling system. All IN939

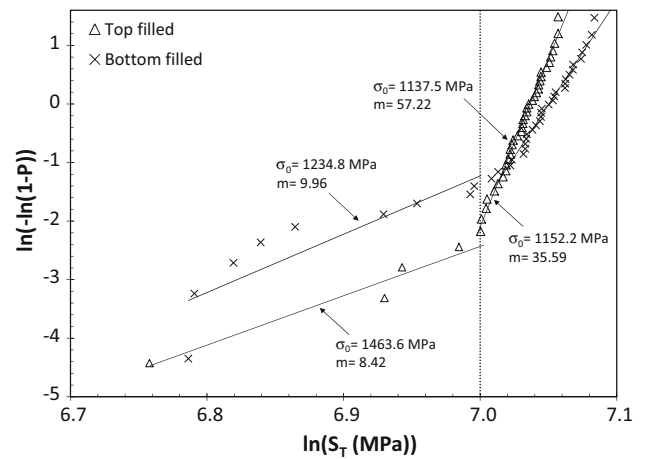


Fig. 2—Reanalysis of the data by Cox *et al.*^[12] on the effect of filling system design on the tensile strength of IN939 alloy castings. Note that 2-parameter Weibull distributions were assumed in each case, as originally used by Cox *et al.*

castings were hot isostatically pressed (HIPed). The Weibull analysis showed that tensile strength data below 1100 MPa had a much lower slope in the Weibull probability plot than those above 1100 MPa. The Weibull probability plots for the data of Cox *et al.* are presented in Figure 2. Note that for both bottom- and top-filled castings, the slope of the best-fit line (hence 2-parameter Weibull is assumed) is significantly less at lower values of tensile strength. Consequently, Cox *et al.* fitted different lines to the two regions, as presented in Figure 2.

The first mixture model was proposed by Weibull^[13] who analyzed the tensile strength of malleable cast iron reported by Pearson^[14] after noticing that 15 of the 75 castings were poured at a different location. For the mixture of distributions, Weibull^[15] suggested the following form:

$$P = pP_1 + (1 - p)P_2, \quad [5]$$

where p is fraction of the Weibull distribution number 1 in the mixture, and subscripts 1 and 2 refer to the two Weibull distributions. The Weibull probability plot for the data of Pearson as well as the values of the estimated parameters are presented in Figure 3.

The statistical treatment of the link between defect size distributions and the resultant Weibull mixture in ceramics was discussed in detail by Johnson.^[16] According to Johnson, Eq. [5] applies only when defect distributions are mutually exclusive, *i.e.*, when fracture is due to one type of flaw (defect). This scenario does not mean that specimens will contain only one type of defect; it may be that one type of defect always “wins” over the other type, and hence, there is no “competition”. When there is indeed some competition between the defect types, the mixture methods are as follows^[17]:

$$P = 1 - (1 - P_1)(1 - P_2) \quad [6]$$

$$P = (1 - p)P_1 + p(1 - (1 - P_1)(1 - P_2)) \quad [7]$$

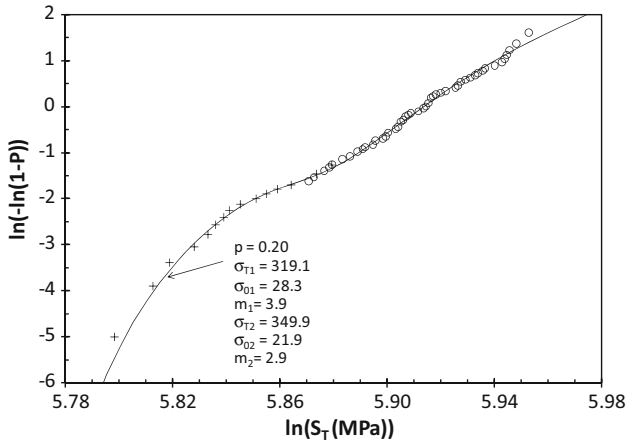


Fig. 3—Reanalysis^[10] of the tensile strength of malleable iron castings as reported by Pearson.^[14]

Equations [6] and [7] are for concurrent and partially concurrent defect distributions, respectively. In the concurrent model, the two defect distributions always coexist and are always in competition to start failure. In the partially concurrent version, defect distribution 1 has no competition in a fraction, p , of the castings and in the rest of the castings ($1 - p$), two distributions are in full competition. The three types of Weibull mixtures are summarized in Table I.

According to Johnson, to determine which kind of Weibull mixture is appropriate, one should (i) identify the types of defects causing the premature fracture on the fracture surfaces, and (ii) determine whether the two defect distributions are competing with each other. Hence the analysis of the fracture surfaces with a scanning electron microscope (SEM) and an intimate knowledge of the casting process are necessary to make the correct selection of the type of Weibull mixture.

To complete the mathematical treatment of the Weibull mixtures, we turn our attention to the probability density functions of Weibull mixtures. Note that the probability density functions for the three types of Weibull mixtures, Eqs. [5] through [7], are found by using Eq. [2a] as:

$$f = pf_1 + (1 - p)f_2 \quad [8]$$

$$f = f_1 + f_2 - f_1P_2 - f_2P_1 \quad [9]$$

$$f = (1 - p)f_1 + p(f_1 + f_2 - f_1P_2 - f_2P_1) \quad [10]$$

for the mutually exclusive, concurrent, and partially concurrent Weibull mixtures, respectively.

B. Multiple Defect Distributions

It has been only recently understood^[18,19] that the degradation of and variability in the mechanical properties of castings are related to the defects that are introduced into the molten metal usually as a result of poor handling of the molten metal and/or poor filling

Table I. Weibull Mixtures for Various Types of Defect Distributions

Defect Distributions	Mixture Method for P and f	Equations for Cumulative Probability
Mutually exclusive (no competition)	$P = pP_1 + (1 - p)P_2$ $f = pf_1 + (1 - p)f_2$	$P = p \left(1 - \exp \left(- \left(\frac{\sigma - \sigma_{01}}{\sigma_{01}} \right)^{m_1} \right) \right) + (1 - p) \left(1 - \exp \left(- \left(\frac{\sigma - \sigma_{02}}{\sigma_{02}} \right)^{m_2} \right) \right)$
Concurrent (full competition)	$P = 1 - (1 - P_1)(1 - P_2)$ $f = f_1 + f_2 - f_1P_2 - f_2P_1$	$P = 1 - \exp \left(- \left(\frac{\sigma - \sigma_{01}}{\sigma_{01}} \right)^{m_1} - \left(\frac{\sigma - \sigma_{02}}{\sigma_{02}} \right)^{m_2} \right)$
Partially concurrent (partial competition)	$P = (1 - p)P_1 + p(1 - (1 - P_1)(1 - P_2))$ $f = (1 - p)f_1 + p(f_1 + f_2 - f_1P_2 - f_2P_1)$	$P = 1 - (1 - p) \exp \left(- \left(\frac{\sigma - \sigma_{01}}{\sigma_{01}} \right)^{m_1} \right) - p \exp \left(- \left(\frac{\sigma - \sigma_{01}}{\sigma_{01}} \right)^{m_1} - \left(\frac{\sigma - \sigma_{02}}{\sigma_{02}} \right)^{m_2} \right)$

system design. These defects, namely bifilms, are incorporated into the bulk of the liquid by an entrainment process, in which the surface oxide folds over itself. In most steel castings, the oxide has a significantly lower density than the metal, and therefore floats to the surface quickly, leaving the metal relatively free of defects. In aluminum alloys, the folded oxide has practically neutral buoyancy, so that defects tend to remain in suspension. The layer of air in the folded oxide can (i) grow into a pore as a result of the negative pressure due to contraction of the solidifying metal and/or rejection of gasses, originally dissolved in liquid metal upon solidification, or (ii) remain as an unbonded surface, like a crack, in the solidified alloy, which usually serves as heterogeneous nucleation sites for inter-metallics.

Prior studies^[20–25] have shown that there are multiple types of defects in castings, including bifilms and pores associated with bifilms. From a process viewpoint, most Weibull plots for mechanical data of the castings can be expected to reveal at least two populations of defects^[10]:

1. The original rather fine scattering of defects remaining in suspension in the originally poured liquid from the crucible or ladle (prior damage). These bifilms, referred to as “old”, have a typical minimum thickness of approximately 10 μm and show only coarse wrinkles.
2. The large new bifilms (new damage) that would have been produced during the pouring if the filling system was not designed properly. These “young” oxides have a minimum thickness of tens of nanometers or less and show fine wrinkles on fracture surfaces of castings.

A single Weibull distribution can normally be expected in castings whose filling systems were designed so that no new damage to liquid metal takes place during filling. However, because the initial melt quality is seldom high, and the filling systems of many castings are poorly designed, multiple defect distributions can be expected to be the norm, rather than the exception, even when the castings are poured in a vacuum.^[26,27] Therefore, it is recommended^[10] that certain process information, such as melt quality and the design of the filling system be taken into account during the Weibull analysis of casting data.

The presence of multiple defect types as failure initiators was demonstrated by Nyahumwa *et al.*^[20] who investigated the effect of placing a 20 ppi foam filter in the filling system on the fatigue life of bottom-filled Al-7 pct Si-Mg alloy castings. SEM analysis of the fracture surfaces showed that the failure-initiating defects were “old” bifilms, “young” bifilms, pores associated with both “young” and “old” bifilms, and slip surfaces. The data of Nyahumwa *et al.*^[20] for filtered and not-filtered castings tested at a maximum stress of 150 MPa, in the form of a cumulative probability plot is presented in Figure 4. Due to the presence of these multiple defect types which coexist in the metal, Nyahumwa *et al.*^[22] used the partially concurrent Weibull mixture to model the fatigue life data for Al-7 pct Si-Mg alloy castings. Wang *et al.*^[25] found similar

results on the fracture surfaces of A356 alloy fatigue specimens after running fatigue tests at a maximum stress of 222 MPa and $R = 0.1$. Wang *et al.*^[25] analyzed the fatigue life distributions separately for every type of failure-initiating defect. Reinterpretations of these datasets will be discussed below.

III. WORKED EXAMPLES OF WEIBULL MIXTURES

For Weibull probability plots to be interpreted correctly, it is the author’s opinion that in addition to the casting process knowledge, one should also incorporate into the analysis the relationship between maximum defect size and the mechanical property of interest. The relationships between defects size distributions and two mechanical properties, namely tensile strength (or elongation) and fatigue life, are discussed below along with case studies by using data from the literature.

A. Weibull Mixtures in Tensile Properties

A relationship between fracture stress, σ_F , and maximum defect size, A_i , was suggested by Gruenberg *et al.*^[28] based on elasto-plastic and linear elastic fracture mechanics, and was applied successfully^[29] to A356 castings for tensile strength and elongation. The effect of defect size distribution on the statistical distribution of tensile strength (S_T) is shown schematically in Figure 5, with the curve showing the relationship suggested by Gruenberg *et al.* Note that elongation (e_F) vs defect size plots show the same trend.^[29] If there are two distinct defect size distributions as shown in Figure 5, the result is a Weibull mixture in the tensile strength (and elongation) of castings.

B. Case Study 1: The Effect of Filtering and Melt Quality on Elongation in A356 Alloy Castings

Eisaabadi *et al.*^[24] investigated the effect of stirring (and therefore melt quality getting progressively impaired by the entrainment of surface film) and the presence (or absence) of a filter in the filling system on the tensile properties of Al-7 pct Si-Mg alloy castings. They had three casting conditions from the same melt: (i) not stirred and filtered, (ii) stirred and not filtered, and (iii) stirred and filtered. A 10 ppi ceramic foam filter was used in those runs where the liquid metal had to go through a filter.

The Weibull probability plots for elongation values are presented in Figure 6(a). Note that the linear trends for conditions “not stirred & filtered” and “stirred & not filtered” in their Weibull probability plots indicate two-parameter Weibull distributions. Data from “stirred & filtered” have two distinct regions with different slopes. Analysis of fracture surfaces *via* SEM, as suggested by Johnson,^[16] showed that all castings, indicated with filled triangles, failed due to the presence of coarse “old” oxides, entrained as a result of intentional stirring, which managed to go through the filter. Those indicated

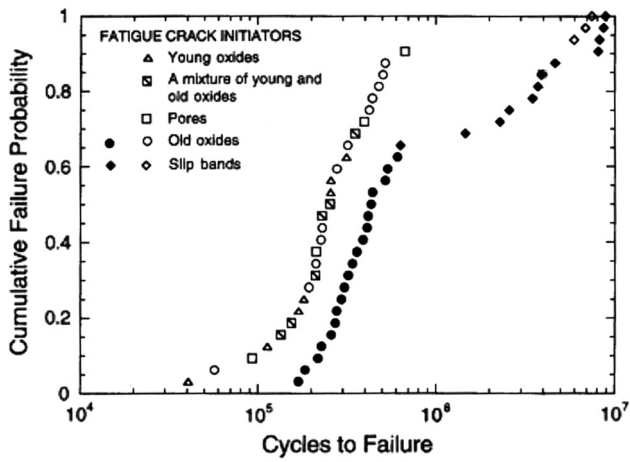


Fig. 4—The cumulative probability plot of fatigue life data of Nyahumwa *et al.*^[20] for not-filtered (hollow symbols) and filtered (full symbols), bottom-filled A356 castings. (Courtesy of Metallurgical and Materials Transactions A).

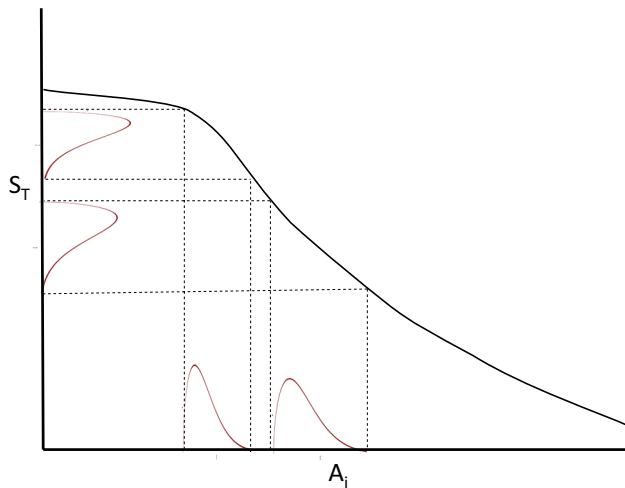


Fig. 5—Schematic illustration of how two different defect size distributions present simultaneously in castings affect the fracture stress distribution.

with hollow triangles, however, had “young” oxides on their fracture surfaces and there were no “old” oxides detected during the SEM analysis (the sizes of oxide bifilms were not measured; only their type was identified). Hence, the filter was effective in some, not all, castings, although the initial melt quality was poor due to stirring. Therefore, the Weibull mixture is due to different defect distributions. It can be argued that the two types of oxide bifilms exist concurrently in the castings that failed at lower elongation (full triangles), but only “young” oxide bifilms are in the casting with higher elongations. Hence the partially concurrent Weibull mixture model presented in Eq. [7] should be applicable. However, there is a significant gap between the lower and upper distributions for elongation. When there is an “old” bifilm in the specimen, there is no competition and “old” bifilm “wins” all the time over

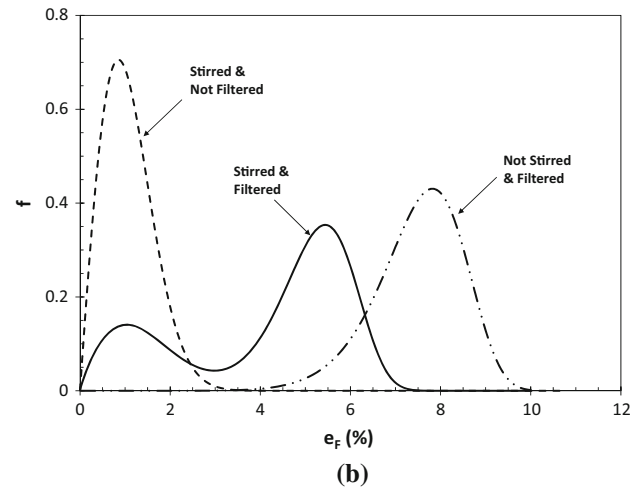
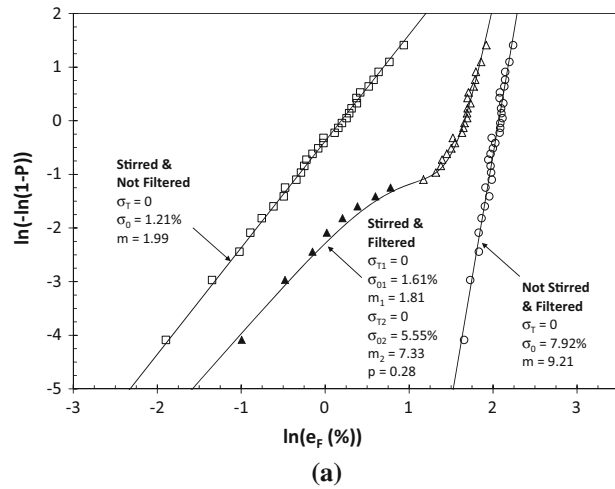


Fig. 6—(a) Weibull probability plots, and (b) probability density functions for elongation of Al-7 pct Si-Mg alloy castings under three conditions.^[24]

“young” oxide bifilms in initiating premature fracture. Therefore, the mutually exclusive version (Eq. [5]) can be used when data from two distributions do not overlap although the defects are partially concurrent in the specimens. It is also significant that tensile strength data showed the same trends as elongation.

As indicated in Figure 6(a), the fraction of the lower Weibull distribution for the stirred & filtered castings is 0.28, which indicates that the filter was only 72 pct effective in catching large, coarse bifilms. This result is identical to the efficiency of a 10 ppi foam filter, reported by Ardekhani and Raiszadeh,^[30] after conducting metallographic analysis and in filtered and unfiltered aluminum castings, and measuring the number density of pores in samples. Hence the procedure followed by Eisaabadi *et al.* and statistical analysis by using Weibull mixtures can be used to measure the efficiency of filters instead of the tedious metallographic analysis.

The probability density functions for Weibull distributions for Eisaabadi *et al.* are plotted in Figure 6(b). It is noteworthy that the location and the scatter in the lower distribution in the Weibull mixture corresponds

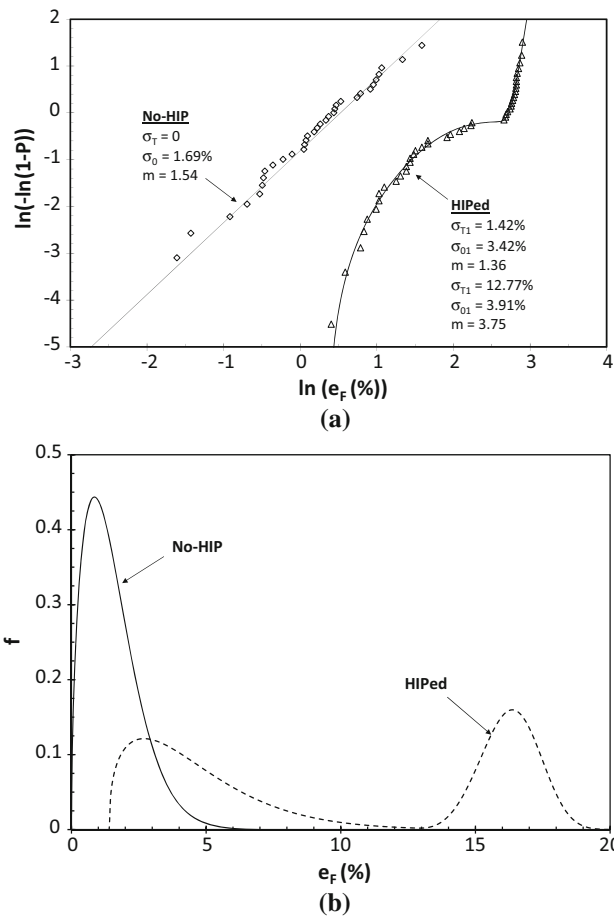


Fig. 7—(a) Weibull probability plots, and (b) probability density functions for elongation of A206 alloy castings in HIPed or no-HIP conditions. [Data from Ref. 31].

exactly to those of “stirred & not filtered”, representing those casting in which the “old” oxide bifilms managed to go through the filter. The upper distribution, however, does not correspond to the distribution for the original condition (“not stirred & filtered”). Hence there is residual damage in those castings due to stirring even when the coarse “old” oxides are trapped in the filter. The residual damage is most probably due to “young” oxides entrained along with the “old” during stirring.

C. Case Study 2: The Effect of HIP on Tensile Properties of A206 Castings

Staley *et al.*^[31] conducted experiments to determine the effectiveness of various HIP conditions on the tensile properties of A206 aluminum alloy castings. Chill cast pig type ingots of A206 were procured for testing since it was expected that ingots produced by conventional processing techniques would exhibit many oxides and much porosity. Specimens were excised from ingots that were either hot isostatically pressed (HIPed) or ingots that did not receive the HIP treatment (no HIP).

Weibull probability plots for elongation in HIPed and no-HIP specimens are presented in Figure 7(a). Note that the data for no-HIP condition has a linear trend,

indicating that the threshold is zero and the size of defects in the castings is large.^[10] Fractographic analysis showed that old spinel ($MgAl_2O_4$) bifilms covered up to 55 pct of the fracture surface of tensile specimens.^[31] For the HIPed condition, there is a Weibull mixture with both distributions having threshold values. Because a positive threshold implies smaller defect sizes,^[10] it can be concluded that HIP treatment reduced the size of the defects in the castings but the effectiveness of the HIP treatment was at two distinct levels, resulting in a Weibull mixture. The two distinct levels of response to HIP treatment is evident in Figure 7(b) in which the probability density functions are plotted.

Analysis of fracture surfaces of tensile specimens *via* SEM showed^[31] that the defects that led to premature failure in no-HIP specimens were “old” and “young” oxides and associated large pores. In HIPed castings, there were no pores, as can be expected. The “old” oxides were found to be resistant to healing and therefore, cracks remained even after the pores around the old oxide bifilms were closed. The lower distribution in HIPed specimens is predominantly due to premature failure from “old” oxide bifilms. The upper distribution represents premature failure due to “young” oxide bifilms that form during pouring and filling of the current casting. The young bifilms, unlike old bifilms, were partially healed during the HIP treatment. Therefore, the upper distribution represents the case where an “old” oxide crack either does not exist in the casting or is parallel to the direction of loading. Hence the mutually exclusive Weibull mixture model (no competition) is applicable in this case. The “old” oxides “win” all the time over partially healed “young” oxides to lead to premature fracture in HIPed castings. Hence it can be concluded that for elongation to be improved significantly by HIP, as represented by the upper distribution in Figure 7(b), the coarse, large “old” oxide films should not be present in the casting.

D. Case 3: Revisiting The Tensile Strength Data of Cox *et al.* for IN939 Castings

The data of Cox *et al.* for IN939 castings, introduced in Figure 2 along with their Weibull fits, were reanalyzed. The Weibull probability plots are presented in Figure 8(a). The estimated parameters for three-parameter Weibull fits are also indicated in Figure 8(a). Note that the lower distribution for bottom-filled castings has a positive threshold value whereas the estimated threshold is zero for the top-filled castings. This finding implies that the defects causing premature failure in the lower distributions are smaller in size for the bottom-filled than for the top-filled castings. Also note that the threshold value is larger in the upper distribution of bottom-filled castings than in top-filled castings. The same interpretation about the defect size can be made for this finding as well. The improvement by bottom filling becomes more obvious in Figure 8(b) in which the probability density functions are plotted. The upper distribution is located at higher values of tensile strength than the distribution after top-filling.

Because Cox *et al.* did not analyze fracture surfaces, we can only speculate the reasons for the two Weibull distributions. Bifilm defects, both “old” and “young”, are not uncommon in Ni-based superalloys.^[26] Coarse bifilms were observed^[26] during the failure analysis in superalloy castings that were subjected to HIP treatment, and it was stated that they seemed almost identical to those observed by Staley *et al.*^[31] Hence, it is conceivable that the lower distributions are probably due to “old” oxides that resisted to healing during the HIP treatment, whereas the upper distributions represent the response (healing) of pores and “young” oxides during the HIP treatment in the absence of “old” bifilms. Therefore the mutually exclusive Weibull mixture is applicable in this case.

Computational fluid dynamics (CFD) modeling^[32] and real-time X-ray observations of top- and bottom-filled investment castings showed^[32,33] that there is much less surface turbulence during filling in bottom-filled investment castings than in the top-filled. Consequently, creation of new surfaces that lead to “young” oxides and their entrainment can be expected to be at a lower rate in bottom-filled castings than in the top-filled. Therefore, the number density of entrained “young” oxide films,

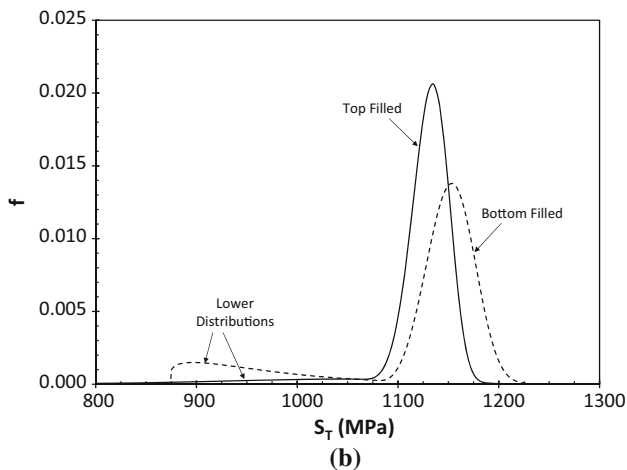
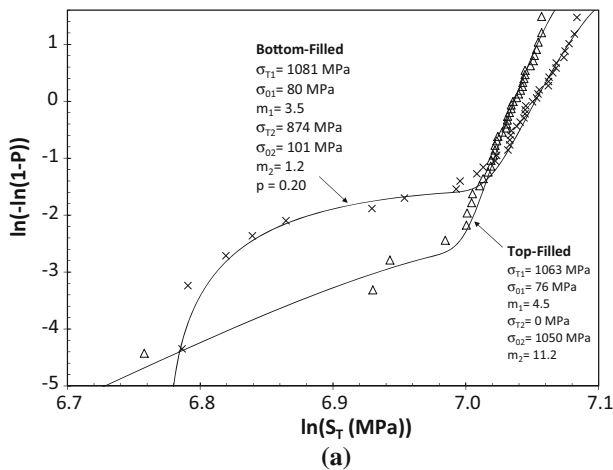


Fig. 8—(a) Weibull probability plots, and (b) probability density functions for tensile strength of bottom- and top-filled IN939 alloy castings. [Data from Ref. 12].

that may partially-heal upon HIP treatment, can be expected to be lower in the bottom-filled castings, leading to increased tensile strength values.

E. Weibull Mixtures in Fatigue Life Data

For a section of a casting that contains a crack-like defect of initial length a_i , the crack length increases to a value, a , at any given number of stress cycles, N . The fatigue crack growth rate in the power-law or steady-state stage, as expressed by the Paris-Erdoğan law,^[34] is written as,

$$\frac{da}{dN} = C(\Delta K_{\text{eff}})^m, \quad [11]$$

where C and m are Paris-Erdoğan constants and ΔK_{eff} is the effective stress intensity factor range. Equation [11] can be integrated and arranged, after simplifying assumptions, to obtain:

$$N_f = N_i + B\sigma_a^{-m} A_i^{\frac{2-m}{4}}, \quad [12]$$

where N_f is cycles until failure (fatigue life), N_i is cycles to initiate a fatigue crack, B is a constant, σ_a is alternating stress amplitude and A_i is the area of the fatigue-initiating defect as measured on the fracture surface. Equation [12] is identical to the equation used in previous studies^[21,35–37] and its derivation is provided in Reference 38. The relationship between A_i and N_f is illustrated schematically in Figure 9. Because $m \approx 4$ in aluminum alloys, the exponent of A_i in Eq. [12] is approximately -0.5 .^[21,37] Similarly, Murakami and Endo^[39,40] used $\sqrt{A_i}$ as a parameter to model the fatigue limit of surface and internal defects in steels. Moreover, they showed that the fatigue strength is governed by one critical inclusion, which usually has the largest size, not by the presence of many inclusions, although most steels were found^[41] to contain multiple inclusion types, with each having their own size distribution.

As noted previously, Weibull mixtures found in the fatigue life data of A356 castings were assumed to be

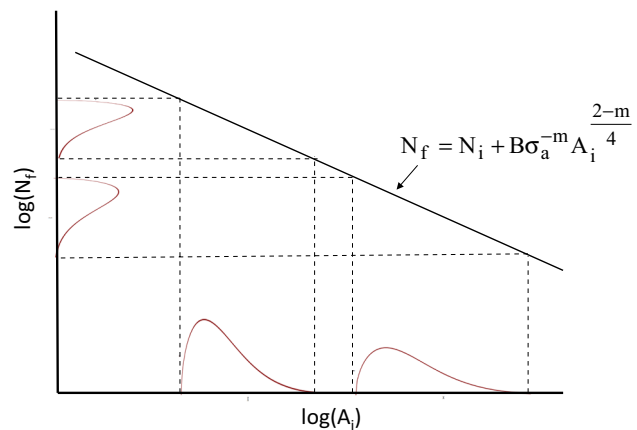


Fig. 9—Schematic illustration between the defect size and fatigue life. The assumption that the Weibull mixture in fatigue life data is due to multiple defects and their distinct size distributions is also indicated.

due to multiple defect types each with their own size distribution.^[22] This assumption is also depicted in Figure 9.

F. Case Study 4: The Effect of HIP on Fatigue Life in A206 Castings

Staley *et al.*^[42] conducted fatigue tests on specimens excised from HIPed and no-HIP A206 aluminum alloy ingots at a maximum stress of 170 MPa and $R = 0.1$. SEM analysis of fracture surfaces of fatigue specimens showed that all fatigue cracks for no-HIP specimens initiated at surface-connected porosity contained various amounts of alumina and spinel bifilms. All fatigue cracks for HIPed specimens were initiated at surface-connected or interior oxides, predominantly “old” oxides.

Weibull probability plots for no-HIP and HIPed conditions are presented in Figure 10.** Note that, as in

**Although natural logarithm of the mechanical property data is used conventionally as the x-axis in Weibull probability plots, for fatigue life data, it is the author’s recommendation that logarithm of data with a base 10 be used for easier interpretation.

the results for elongation (discussed above), fatigue life data follow a single Weibull distribution, whereas after HIP treatment, fatigue life data indicate a Weibull mixture. The lower distribution is for fatigue initiation at surface defects and the upper distribution is for fatigue initiation at defects in the interior. By eliminating the pores, fatigue life increases by more than an order of magnitude even when fatigue crack is initiated at the specimen surface. The improvement is at least two orders of magnitude when the fatigue crack is initiated in the interior.

Fatigue crack initiation from subsurface (interior) defects has received considerable attention recently.^[43–49] The S–N curve for the subsurface defects is different from the one for those on the surface, as shown schematically in Figure 11. The location of the S–N curve for internal defects will depend on the size of the

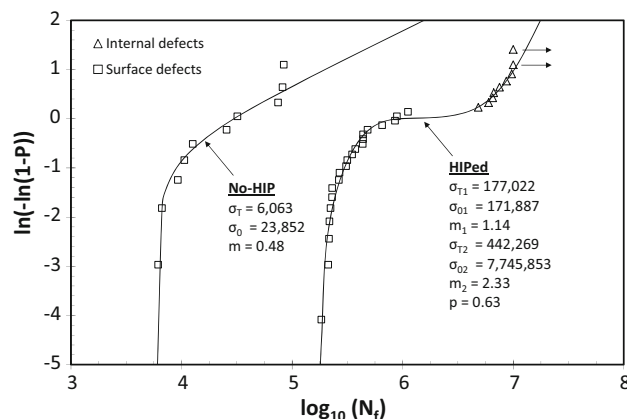


Fig. 10—Reanalysis of fatigue life data by Staley *et al.*^[42] by Weibull probability plots.

internal defect.^[50] Separate S–N curves for surface and subsurface defects were found^[47] for a cast Al-10 pct Si-4 pct Cu-0.6 pct Mg alloy when specimens were subjected to a surface treatment. In several studies, cracks were observed to grow from casting defects at or shortly after the first stress cycle^[51–53] and therefore, N_i in Eq. [12] is often assumed to be zero. However in cases where there is no defect on the surface large enough to initiate a propagating crack, fatigue crack initiation from a subsurface defect takes significantly longer to initiate, resulting in increased fatigue life. When fatigue life data are from a set of castings, some of which have defects on their surfaces while the rest have only subsurface defects, we can expect to have two fatigue life distributions.

G. Case Study 5: Failure-Initiating Defects and Fatigue Life in A356 Castings

In this case study, we will use results from two different studies referred to earlier, by Nyahumwa *et al.*^[20,22] and Wang *et al.*^[25] Nyahumwa *et al.* investigated the effect of placing a 20 ppi filter in the filling system on the fatigue life variability in A356 aluminum alloy castings. Fatigue tests were performed at a maximum stress of 150 and 240 MPa and $R = 0.1$. The fatigue life results as well as the types of fatigue failure-initiating defects determined by SEM analysis were presented in Figure 4. The Weibull probability plots for the not-filtered and filtered castings are presented in Figure 12(a). For the not-filtered castings, the three types of fatigue failure-initiating defects, namely pores, young oxides and old oxides, all follow the same Weibull distribution for the lower fatigue life values. This is significant because three different types of defects seem to have the same effect on fatigue life when they are connected to, or within a close distance to, the specimen surface. Therefore, it is not necessary to treat the three types of defects separately as Nyahumwa *et al.*^[22] did by using the partially concurrent Weibull mixture model (Eq. [7]). Note that there is a large gap in the fatigue life data between the lower and upper distributions. The upper distributions were originally

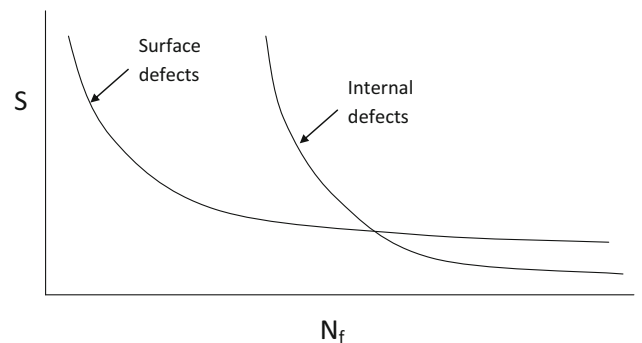


Fig. 11—Schematic illustration of S–N curves of fatigue tested specimens failed from cracks initiated at surface and internal (subsurface) defects.

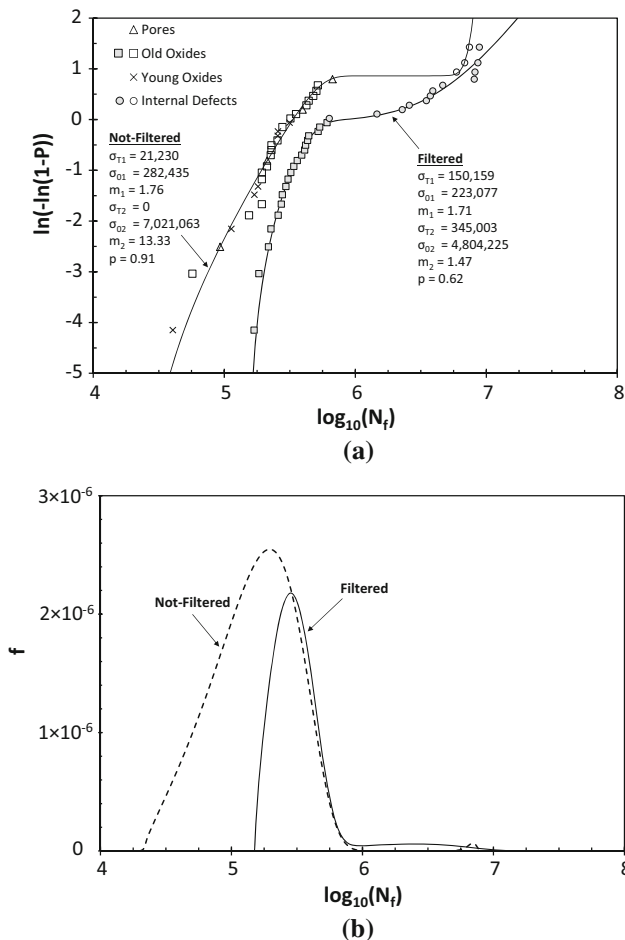


Fig. 12—(a) Weibull probability, and (b) probability density plots for the filtered and not-filtered A356 aluminum alloy castings [Data from Ref. 20, 56].

attributed to slip planes by Nyahumwa *et al.* who later suggested^[54] that slip planes represented defect-free failure, and therefore, the fatigue life potential of cast aluminum alloys was several orders of magnitude higher than the values usually obtained in fatigue tests. Tiryakioğlu *et al.*^[55] reanalyzed fracture surfaces in Nyahumwa's thesis^[56] and concluded that slip planes that were originally considered to be defect-free failure were in fact facets that formed as a result of stress concentrations due to internal defects. These stress concentrations form slip bands in the metal surrounding the defect. However, the root cause for the facet (or slip band) is still a defect, such as a pore or entrained oxide film. Therefore, just as in the dataset for A206 castings by Staley *et al.*, the upper distributions for both not-filtered and filtered castings represent fracture due to internal defects. Because there is no competition, a surface defect would win over a subsurface defect to initiate a fatigue fracture, the mutually exclusive Weibull mixture is more appropriate than the partially concurrent model originally used by Nyahumwa *et al.*

It is noteworthy that the lower distribution in filtered castings represents fatigue fractures that are initiated at old oxide films. Filters are expected to stop the coarse

old oxides. It has been discussed above that filters do allow old bifilms to pass through. In the process of passing through the filter, old bifilms are “chopped”^[57] to smaller pieces, leading to a shift in the size distribution of old oxides to lower values. This point becomes more apparent on the probability density plots for the not-filtered and filtered castings, as shown in Figure 12 (b). The lower tail of the lower distribution shifts to higher values whereas the upper tails are almost identical. Hence, the largest defects on the specimen surface get smaller in size with the filter in the filling system. A reduction in the size of the defects can be expected to increase the probability that a defect will not be connected to the surface,^[58] and therefore will be subsurface and lead to longer fatigue life. That is probably why the fraction of fatigue failures that initiated from internal defects is significantly higher in castings.

Wang *et al.* investigated the fatigue life variability in A356 alloy castings and determined the type of fatigue crack initiating defects for each casting. Some specimens were subjected to a HIP treatment to close pores, although the specific specimens that were HIPed were not disclosed in the paper. Fatigue failures were attributed to three different types of defects; pores, oxides, and slip planes. Wang *et al.* presented separate Weibull probability plots due to these three fatigue crack initiators. The data of Wang *et al.* and the original two-parameter Weibull fits are presented in Figure 13 (a). Note that in all three cases, the data at lower values deviate from the linear fit in a manner which strongly suggest that $\sigma_T > 0$. It should be noted that pores and oxides, as reported by Wang *et al.*, were all connected to the surface of fatigue specimens. Moreover, slip steps were observed around defects when the fatigue-initiating defects were not connected to the surface. These internal defects were surrounded by the slip planes and therefore, the fatigue initiators were still defects, such as oxides, which were subsurface. When all data are plotted on the same Weibull probability plot, Figure 13(b), it becomes evident that fatigue life data with pores and oxides on the surface come from the same Weibull distribution. Specimens that initiated cracks internally, the fatigue life has a distinctly different Weibull distribution. As in the cases of A206 castings by Staley *et al.* and A356 castings by Nyahumwa *et al.*, there is no competition between surface and interior defects because surface defects dominate over to initiate fatigue failure. Hence the mutually exclusive Weibull mixture is most suitable for this case.

All three datasets for fatigue life with Weibull mixtures showed that the lower distribution represents failure due to surface defects and upper distribution due to internal defects. Because pores, young and old bifilms are all attributed to entrainment of the surface film, it is conceivable to treat pores and bifilms together as “entrainment defects”. Moreover, taking Figure 11 into account, the original assumption of multiple defect size distributions as the source of Weibull mixtures, as depicted in Figure 9, is false. A modified version is presented in Figure 14 in which a single defect size distribution leads to a Weibull mixture in fatigue life

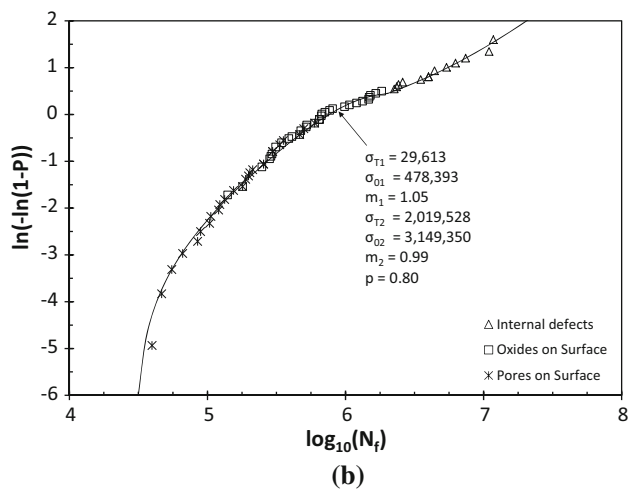
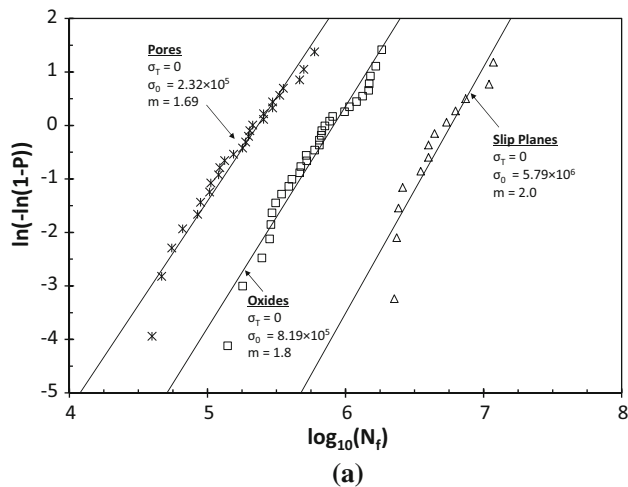


Fig. 13—Reanalysis of data by Wang *et al.*^[25] Weibull probability plots for fatigue life (a) for three different fatigue crack initiators based on original classifications by Wang *et al.*, and (b) after all data are combined and slip planes are interpreted as indications of internal defects.

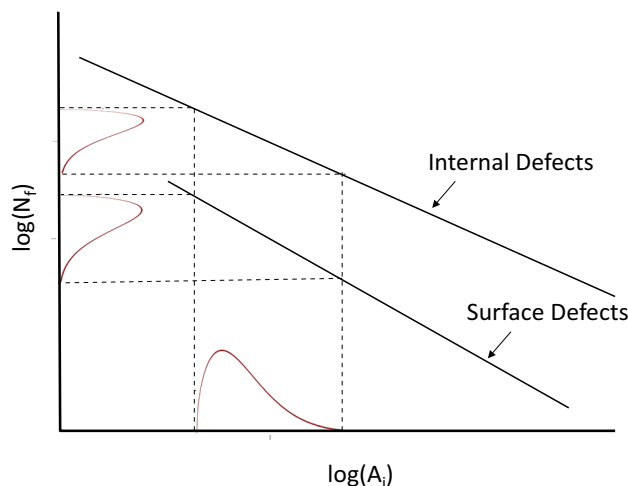


Fig. 14—Schematic illustration of a single defect size distribution leading to a Weibull mixture when two failure mechanisms are active.

when two failure mechanisms, *i.e.*, due to surface and interior defects, are active. More in-depth discussion of Figure 14 along with experimental data is given in Reference 55.

IV. CONCLUSIONS

1. When Weibull plots are interpreted, the possible presence of Weibull mixtures can be detected by inflection points in the trend of the data. The actual presence of Weibull mixtures should still be validated through the analysis of fracture surfaces.
2. In tensile data, Weibull mixtures are due to two distinct defect distributions: “old” and “young” bifilms, which are a result of prior processing and mold filling, respectively. “Old” bifilms are the predominant defect and result in the lower distribution, whereas “young” bifilms results on the upper distribution.
3. In fatigue life data, Weibull mixtures are due to two failure mechanisms being active: failure due to cracks initiating from surface defects and interior defects. Surface defects are predominant and interior defects cause fatigue failure only when there are no cracks initiated by surface defects.
4. Fatigue fracture from different defect types such as “old” and “young” bifilms and pores were characterized separately in several studies in the literature. Reanalysis of the data from those studies showed that fatigue life data from different defect types belong to the same distribution. Hence it is not necessary to analyze different defects separately. The only distinction comes from whether the defect is on the surface of the specimen.
5. In all cases presented in this study, only the mutually exclusive Weibull mixture was applicable. The author has yet to come across a case in which either the concurrent and partially concurrent Weibull mixture would be applicable.

REFERENCES

1. A.A. Griffith: *Philos. Trans. R. Soc. Lond. Ser. A*, 1921, vol. 221, pp. 163–98.
2. P.F. Thomason: *Ductile Fracture of Metals*, Pergamon Press, Oxford, 1990.
3. J.F. Knott: in *Recent Advances in Fracture*, R.K. Mahidhara, ed., TMS, Warrendale, PA, 1997.
4. B. Epstein: *J. Am. Stat. Assoc.*, 1948, vol. 43, pp. 403–12.
5. F.T. Pierce: *J. Text. Inst.*, 1926, vol. 17, pp. T355–68.
6. T.T. Shih: *Eng. Fract. Mech.*, 1980, vol. 13, pp. 257–71.
7. W. Weibull: *J. Appl. Mech.*, 1951, vol. 13, pp. 293–97.
8. N.R. Green and J. Campbell: *Mater. Sci. Eng. A*, 1993, vol. A173, pp. 261–66.
9. N.R. Green and J. Campbell: *AFS Trans.*, 1994, vol. 102, pp. 341–47.

10. M. Tiryakioğlu and J. Campbell: *Metall. Mater. Trans. A*, 2010, vol. 41A, pp. 3121–29.
11. S. Jiang and D. Keçecioglu: *IEEE Trans. Reliab.*, 1992, vol. 41, pp. 241–47.
12. M. Cox, M. Wickins, J.P. Kuang, R.A. Harding, and J. Campbell: *Mater. Sci. Technol.*, 2000, vol. 16, pp. 1445–52.
13. W. Weibull: *Proc. The Royal-Swedish Institute for Engineering Research. Nr. 151*, 1939.
14. E.S. Pearson: “The Application of Statistical Methods to Industrial Standardisation and Quality Control”, *British Standard No. 600*, 1935.
15. W. Weibull: *The Phenomenon of Rupture in Solids*, Royal Swedish Institute of Engineering Research (Ingenioersvetenskaps Akad. Handl.), Stockholm, vol. 153, pp. 1–55, 1939.
16. C.A. Johnson: *Fract. Mech. Ceram.*, 1983, vol. 5, pp. 365–86.
17. C.D. Tarum: SAE Technical Paper, 1999-01-0055, 1999.
18. J. Campbell: *Castings*, 2nd ed., Elsevier, Oxford, 2003.
19. J. Campbell: *Mater. Sci. Technol.*, 2006, vol. 22, pp. 127–45, 999–1008.
20. C. Nyahumwa, N.R. Green, and J. Campbell: *Metall. Mater. Trans. A*, 2001, vol. 32A, pp. 349–58.
21. Q.G. Wang, C.J. Davidson, J.R. Griffiths, and P.N. Crepeau: *Metall. Mater. Trans. B*, 2006, vol. 37B, pp. 887–95.
22. C. Nyahumwa, N.R. Green, and J. Campbell: *AFS Trans.*, 1998, vol. 106, pp. 215–23.
23. B. Zhang, D.R. Poirier, and W. Chen: *Metall. Mater. Trans. A*, 1999, vol. 30A, pp. 2659–66.
24. G. Eisaabadi, B.P. Davami, S.K. Kim, and M. Tiryakioğlu: *Mater. Sci. Eng. A*, 2013, vol. 579, pp. 64–70.
25. Q.G. Wang, D. Apelian, and D.A. Lados: *J. Light Met.*, 2001, vol. 1, pp. 73–84.
26. J. Campbell and M. Tiryakioğlu: *Metall. Mater. Trans. B*, 2012, vol. 43B, pp. 902–14.
27. A.K.M.B. Rashid and J. Campbell: *Metall. Mater. Trans. A*, 2004, vol. 35A, pp. 2063–71.
28. K.M. Gruenberg, B.A. Craig, B.M. Hillberry, R.J. Bucci, and A.J. Hinkle: *Int. J. Fatigue*, 2004, vol. 26, pp. 615–27.
29. M. Tiryakioğlu: *Mater. Sci. Eng. A*, 2010, vol. A527, pp. 4546–49.
30. A. Ardekhani and R. Raiszadeh: *J. Mater. Eng. Perform.*, 2012, vol. 21, pp. 1352–62.
31. J.T. Staley, Jr., M. Tiryakioğlu, and J. Campbell: *Mater. Sci. Eng. A*, 2007, vol. 460–461, pp. 324–34.
32. M. Cox, R.A. Harding, and J. Campbell: *Mater. Sci. Technol.*, 2003, vol. 19, pp. 613–25.
33. D.Z. Li, J. Campbell, and Y.Y. Li: *J. Mater. Process. Technol.*, 2004, vol. 148, pp. 310–16.
34. P. Paris and F. Erdoğan: *J. Basic Eng.*, 1963, vol. 85, pp. 528–34.
35. M.A. Przystupa, R.J. Bucci, P.E. Magnusen, and A.J. Hinkle: *Int. J. Fatigue*, 1997, vol. 19, pp. S285–88.
36. M.J. Couper, A.E. Neeson, and J.R. Griffiths: *Fatigue Fract. Eng. Mater. Struct.*, 1990, vol. 13, pp. 213–27.
37. C.J. Davidson, J.R. Griffiths, and A.S. Machin: *Fatigue Fract. Eng. Mater. Struct.*, 2002, vol. 25, pp. 223–30.
38. M. Tiryakioğlu: *Metall. Mater. Trans. A*, 2009, vol. 40A, pp. 1623–30.
39. Y. Murakami and M. Endo: *Int. J. Fatigue*, 1994, vol. 16, pp. 163–82.
40. Y. Murakami: *JSME Int. J.*, 1989, vol. 32, pp. 167–80.
41. S. Beretta and Y. Murakami: *Metall. Mater. Trans. B*, 2001, vol. 32B, pp. 517–23.
42. J.T. Staley, Jr., M. Tiryakioğlu, and J. Campbell: *Mater. Sci. Eng. A*, 2007, vol. 465, pp. 136–45.
43. O. Umezawa, K. Nagai, and K. Ishikawa: *Tetsu to Hagane*, 1989, vol. 75, pp. 159–66.
44. H. Mughrabi: *Fatigue Fract. Eng. Mater. Struct.*, 2002, vol. 25, pp. 755–64.
45. K. Sadananda, A.K. Vasudevan, and N. Phan: *Int. J. Fatigue*, 2007, vol. 29, pp. 2060–71.
46. C. Przybyla, R. Prasannavenkatesan, N. Salajegheh, and D.L. McDowell: *Int. J. Fatigue*, 2010, vol. 32, pp. 512–25.
47. Y. Nakamura, T. Sakai, H. Hirano, and K.S. RaviChandran: *Intl. J. Fatigue*, 2010, vol. 32, pp. 621–26.
48. C. Bathias: *Fatigue Fract. Eng. Mater. Struct.*, 1999, vol. 22, pp. 559–65.
49. Q.Y. Wang, J.Y. Berard, A. Dubarre, G. Baudry, S. Rathery, and C. Bathias: *Fatigue Fract. Eng. Mater. Struct.*, 1999, vol. 22, pp. 667–72.
50. O. Umezawa and K. Nagai: *ISIJ Int.*, 1997, vol. 37, pp. 1170–79.
51. B. Skallerud, T. Iveland, and G. Härkegård: *Eng. Fract. Mech.*, 1993, vol. 44, pp. 857–74.
52. S.A. Barter, L. Molent, N. Goldsmith, and R. Jones: *J. Eng. Fail. Anal.*, 2005, vol. 12, pp. 99–128.
53. B.R. Crawford, C. Loader, A.R. Ward, C. Urbani, M.R. Bache, S. H. Spence, D.G. Hay, W.J. Evans, G. Clark, and A.J. Stonham: *Fatigue Fract. Eng. Mater. Struct.*, 2005, vol. 28, pp. 795–808.
54. C. Nyahumwa, N.R. Green, and J. Campbell: *J. Mech. Behav. Mater.*, 1998, vol. 9, pp. 227–35.
55. M. Tiryakioğlu, J. Campbell, and C. Nyahumwa: *Metall. Mater. Trans. B*, 2011, vol. 42B, pp. 1098–1103.
56. C.W.M. Nyahumwa: Ph.D. Thesis, University of Birmingham, U.K., 1997.
57. B. Sirrell and J. Campbell: *AFS Trans.*, 1997, vol. 105, pp. 645–654.
58. M. Tiryakioğlu: *Mater. Sci. Eng. A*, 2014, vol. A601, pp. 116–22.